The First Structurally Authenticated Organomercury(1+) Thioether Complexes − Mercury−Carbon Bond Activation Related to the Mechanism of the Bacterial Enzyme Organomercurial Lyase

Michaela Wilhelm,[a][‡] Stefan Deeken,[a] Eva Berssen,[a] Wolfgang Saak,[a] Arne Lützen,[a] Rainer Koch,[a] and Henry Strasdeit*[b]

Keywords: Bioinorganic chemistry / Enzyme models / Ligand effects / Mercury / S ligands

The new compounds [MeHg([9]aneS$_3$)](BF$_4$) (**1**), [MeHg([12]aneS$_3$)](BF$_4$) (**2**), and [(MeHg)$_2$([14]aneS$_4$)](BF$_4$)$_2$ (**3**) have been prepared and their crystal structures determined. In **1**, the thioether acts as a tridentate ligand [Hg–S 2.611(2)–2.768(2) Å] and thus the metal atom is tetrahedrally coordinated, which is rare in organomercury chemistry. Temperature-dependent ^{1}H and ^{13}C NMR spectra showed that this coordination is retained in acetonitrile solution. In crystalline **2** and **3**, linear-coordinated Hg^{II} occurs with Hg–S bond lengths of 2.441(4) and 2.425(2) Å. [MeHg([9]aneS$_3$)]$^+$ was found to be stable towards ligand substitution by $CF_3SO_3^-$ in dimethyl sulfoxide, whereas the thioether was partly displaced by $CF_3CO_2^-$ and completely by $CH_3CO_2^-$. Protonolysis by the very strong Brønsted acid CF_3SO_3H in [D$_3$]nitromethane transformed the methanido ligand into methane. The degree of Hg–C bond cleavage was ca. 25% for the four-coordinate [MeHg([9]aneS$_3$)]$^+$ after 1 h, whereas no reaction was observed for two-coordinate [MeHg(SEt$_2$)]$^+$ or MeHgCl under similar conditions even after 24 h. The product Hg^{2+} was trapped as [Hg([9]aneS$_3$)$_2$]$^{2+}$, which is a six-coordinate complex, as shown by a crystal structure analysis of [Hg([9]aneS$_3$)$_2$](BF$_4$)$_2$·2 CH$_3$CN. Quantum chemical calculations [MP2/SDD + SDD ECP Hg, 6-31+G(d,p) other elements] confirmed that hydrogen transfer activation barriers are significantly lower for "high"-coordinate (CN > 2) complexes. Hg–C bond activation by the enzyme organomercurial lyase is possibly also based on multiple (cysteinyl) sulfur ligation. We propose a hypothetical reaction mechanism that involves an OH-containing amino acid side chain or a water molecule simultaneously serving as a proton acceptor (from Cys–SH) and donor (to R$^-$ of RHg$^+$). This mechanism is supported by quantum chemical calculations on a model system.

Introduction

The high toxicity of various mercury compounds is a constant issue of environmental and public health concern. Consequently, the global cycle of mercury, including the considerable effects of anthropogenic activities, has been intensely studied.[1−6] It was found that in the marine environment, the reduction of inorganic mercury (Hg^{2+}) to the elemental form (Hg^0), and the biomethylation of Hg^{2+} to methylmercury ($MeHg^+$) and dimethylmercury ($HgMe_2$) are major reactions. While Hg^0 is released into the atmosphere where it represents the dominant transport form of mercury, methylmercury is partly incorporated by plankton species and accumulates in the food chain, especially in predatory fish.[7,8] Methylmercury is known to be an extreme neurotoxin.[9−16] A recent study estimates that in the USA alone, over 60,000 children are born each year at risk of neurological problems caused by in utero exposure to methylmercury.[9,17]

One of the main factors responsible for the facile biomagnification of methylmercury in the food chain is the relatively high stability of the Hg−CH_3 bond under physiological conditions.[18,19] It is therefore interesting that the bacterial enzyme organomercurial lyase or MerB (gene: *merB*) is capable of accelerating the protonolytic cleavage of methylmercury and other RHg^+ cations by a factor of 10^6-10^7.[20] The products of the enzymatic reaction are the hydrocarbon RH and Hg^{2+} which is eventually complexed by exogenous thiolates. Organomercurial lyase is part of a broad-spectrum mercury resistance system in which a second enzyme, termed mercuric reductase or MerA (gene: *merA*), catalyzes the reduction of Hg^{2+} to Hg^0 with the latter finally diffusing out of the bacterial cell.[21−26] The

[a] Institut für Reine und Angewandte Chemie der Universität Oldenburg
Carl-von-Ossietzky-Str. 9−11, 26129 Oldenburg, Germany
Fax: (internat.) + 49-(0)441-798-3329
[b] Institut für Chemie der Universität Hohenheim
Garbenstr. 30, 70593 Stuttgart, Germany
Fax: (internat.) + 49-(0)711-459-3950
E-mail: h-strasd@uni-hohenheim.de
[‡] Present address: Universität Bremen FB 4/IW3, Keramische Werkstoffe und Bauteile
Am Biologischen Garten 2, 28359 Bremen, Germany

three-dimensional structure and the enzymatic mechanism of organomercurial lyase are still unknown. However, a general mechanistic hypothesis proposed by Walsh and coworkers is available.[20,27] One of its key features is the coordination of the substrate RHg^+ to one or two cysteinyl-S^- groups, enhancing the polarity of the Hg−C bond. A Brønsted-acidic group of the enzyme, possibly a cysteinyl-SH, is thought to be the proton donor in the subsequent protonolysis step (for further details see Results and Discussion). In model studies, Barbaro et al. have demonstrated that a high "primary" coordination number of mercury can contribute to the activation of Hg−C bonds. They found that the tetrahedral phosphane complexes $[RHg\{N(CH_2CH_2PPh_2)_3\}]^+$ (R = Me, Ph) were unusually susceptible to protonolytic Hg−C bond cleavage.[28,29] Results of a theoretical study, comparing Hg−C bond cleavage in $[MeHg(PH_3)]^+$ and $[MeHg(PH_3)_3]^+$, agreed with the experimental observations.[30] Metal ion coordination by phosphanes, however, is "non-physiological". Synthetic analogues that more closely mimic the proposed substrate binding by organomercurial lyase are lacking.

In this paper we describe methylmercury(1+) thioether complexes with properties relevant to the suggested mechanism of organomercurial lyase. Our experimental and theoretical study addresses, among other things, the question of Hg−C bond activation by multiple sulfur ligation. Perhaps surprisingly, $MeHg^+$−thioether complexes have low thermodynamic stabilities with typical log *K* values for the formation of 1:1 complexes falling in the range −1 to 2.[31,32] In marked contrast, the stability constants of thioether complexes of Hg^{2+} are by about ten orders of magnitude larger (log *K* = 8−12).[33] This difference may be attributed to "anti-symbiosis" which means that the soft methanido ligand reduces the affinity of mercury(II) for another soft ligand in the *trans* position.[34] So far, only a few organomercury(1+) thioether complexes have been isolated[35] and, to the best of our knowledge, no crystal structures have been determined.[36] In the following, we report the syntheses and X-ray crystal structures of three new $MeHg^+$ complexes with meso- and macrocyclic thioether ligands. Part of this work has been communicated previously.[37]

Results and Discussion

Syntheses of the Methylmercury Complexes

A suitable methylmercury starting compound was obtained by treating methylmercury hydroxide with a slight excess of tetrafluoroboric acid in aqueous solution. After removal of the solvent, a colorless oil remained. It is known that in strongly acidic aqueous solutions $[MeHg(OH_2)]^+$ is by far the main $MeHg^+$ species.[38] It therefore seemed safe to assume that the obtained product was $[MeHg(OH_2)](BF_4)\cdot xH_2O$. The complex $[MeHg(OH_2)]^+$ should have a similar structure to $[MeHg(DMSO)]^+$, which contains *O*-coordinated dimethyl sulfoxide in solution as well as in the solid state.[39]

In tetrahydrofuran or acetonitrile/diethyl ether, the thioethers [9]aneS$_3$, [12]aneS$_3$, and [14]aneS$_4$ are capable of displacing the aqua ligand from $[MeHg(OH_2)]^+$ {Equation (1); L = [9]aneS$_3$ or [12]aneS$_3$: *n* = 1; L = [14]aneS$_4$: *n* = 2}.

$$n\,[MeHg(OH_2)](BF_4) + L \rightarrow [(MeHg)_nL](BF_4)_n + n\,H_2O \qquad (1)$$

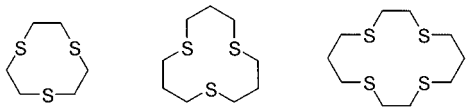

[9]aneS$_3$ [12]aneS$_3$ [14]aneS$_4$

By this route, we prepared the new coordination compounds $[MeHg([9]aneS_3)](BF_4)$ (**1**), $[MeHg([12]aneS_3)](BF_4)$ (**2**), and $[(MeHg)_2([14]aneS_4)](BF_4)_2$ (**3**). They were isolated as analytically pure, crystalline solids in yields of 85% (**1**), 68% (**2**), and 92% (**3**), respectively. We did not succeed in preparing complexes with different numbers of $MeHg^+$ cations per ligand molecule by variation of the starting material ratios. NMR experiments showed, however, that [12]aneS$_3$ can probably bind more than one $MeHg^+$ group (see below). Compounds **1**−**3** are air-stable and soluble in strongly polar organic solvents such as acetonitrile, nitromethane, and dimethyl sulfoxide.

Crystal Structures of Compounds 1−3

Crystals of $[MeHg([9]aneS_3)](BF_4)$ (**1**) consist of discrete $[MeHg([9]aneS_3)]^+$ cations and BF_4^- anions. The compound crystallizes with two formula units in the asymmetric unit. The two symmetry-independent $[MeHg([9]aneS_3)]^+$ complexes have essentially the same structure (Figure 1). Each of the Hg atoms is in a distorted tetrahedral coordination environment formed by a methanido and a tridentate thioether ligand.[29] One Hg−S bond is shorter than the other two. Nevertheless, all three are "primary" bonds. The shortest Hg−S bond is involved in the largest S−Hg−C angle [complex **1**: 142.7(4)°; complex **2**: 136.4(4)°], demonstrating a slight distortion towards the linear coordination usually preferred in RHg^+ complexes. As expected, the mean Hg−S bond length of the four-coordinate complexes in **1** (2.71 Å) is considerably larger than the Hg−S bond lengths of the two-coordinate complexes in **2** [2.441(4) Å] and **3** [2.425(2) Å]. The Hg−C bond lengths are, however, not significantly different [**1**: 2.080(8), 2.075(8) Å; **2**: 2.11(2) Å; **3**: 2.068(7) Å] and correspond well with the average value of 2.07 Å that was derived from a large number of $MeHg^+$ compounds.[29b] As in the free form,[40] the ligand [9]aneS$_3$ in **1** adopts the [333] conformation.[41,42] Coordination to the $MeHg^+$ group resulted in a small increase of the mean transannular S···S distance from 3.451(2) to 3.489 Å and a decrease of the mean S−C−C−S torsion angle from 58.5 to 56.0°. The maximum change of an individual torsion angle was −4.4° at a C−C bond and +4.6° at an S−C bond.

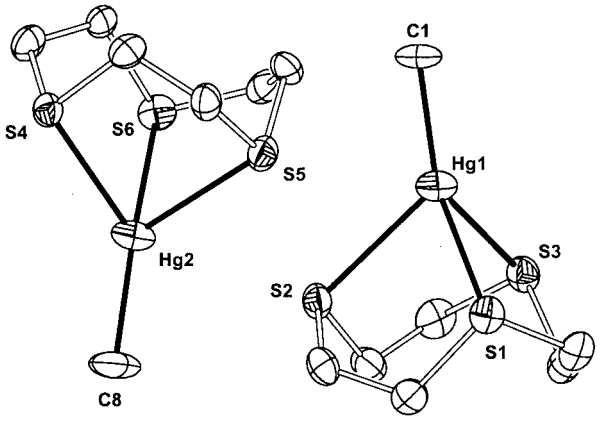

Figure 1. Ellipsoid plot (50% probability level) of the two symmetry-independent $[MeHg([9]aneS_3)]^+$ complexes in **1** showing their mutual orientation in the crystal (hydrogen atoms are omitted); bond lengths [Å] and angles [°]: Hg1−S1 2.611(2), Hg1−S2 2.768(2), Hg1−S3 2.760(2), Hg1−C1 2.080(8), Hg2−S4 2.720(2), Hg2−S5 2.732(2), Hg2−S6 2.677(2), Hg2−C8 2.075(8); S1−Hg1−S2 81.1(1), S1−Hg1−S3 79.6(1), S2−Hg1−S3 79.0(1), S1−Hg1−C1 142.7(4), S2−Hg1−C1 124.9(3), S3−Hg1−C1 127.3(4), S4−Hg2−S5 79.9(1), S4−Hg2−S6 80.4(1), S5−Hg2−S6 80.4(1), S4−Hg2−C8 132.2(3), S5−Hg2−C8 126.6(4), S6−Hg2−C8 136.4(4)

In contrast to the rare tetrahedral coordination observed in **1**, the much more common diagonal coordination of the Hg atom[29] occurs in $[MeHg([12]aneS_3)](BF_4)$ (**2**) and $[(MeHg)_2([14]aneS_4)](BF_4)_2$ (**3**). In addition to the Hg−S and Hg−C "primary" bonds, however, intermolecular "secondary" bonds to the S and F atoms exist in crystals of **2** and **3** (Figures 2 and 3). The sum of the van der Waals radii (R_{vdW}) of the participating atoms usually serves as reference point for establishing the presence of such weak metal−ligand bonds. The R_{vdW} values of Hg^{II} (1.75 Å),[43] S (1.60−2.03 Å), and F (1.30−1.38 Å)[44] give Hg···S and Hg···F van der Waals distances of 3.35−3.78 Å and 3.05−3.13 Å, respectively. The three intermolecular contacts in **2** i.e. two Hg···S and one Hg···F, are below the lower ends of these ranges. In **3**, two Hg···F contacts are at least 0.10 Å shorter than the minimum van der Waals distance. The respective S−Hg···X and C−Hg···X angles (X = S, F) fall within a range reasonable for Hg···X bonding interactions [76.6(4)−101.4(6)°]. Small distortions from linearity of the S−Hg−C angles [**2**: 168.1(6)°; **3**: 174.7(2)°] may be attributed to the influence of the "secondary" bonds. Compared with the free ligand molecules,[45,46] the basic conformations of $[12]aneS_3$ and $[14]aneS_4$ ([3333] and [3434], respectively)[41] are retained in the $MeHg^+$ complexes. The maximum change of a torsion angle between the free and the coordinated forms amounts to ±6−7° both for $[12]aneS_3$ (at S−C) and $[14]aneS_4$ (at S−C and C−C).[47] $[14]aneS_4$ in **3**, as in the free form, possesses a crystallographically imposed center of symmetry.

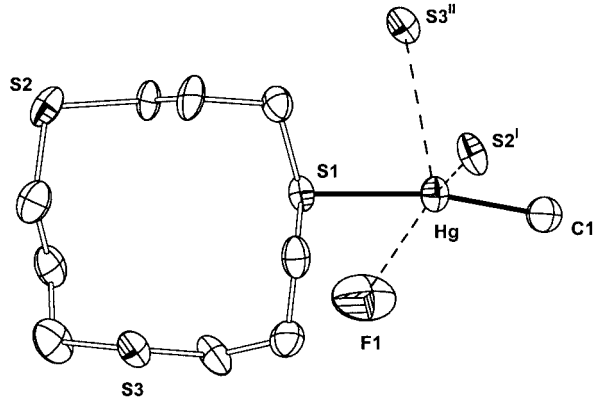

Figure 2. Ellipsoid plot (50% probability level) of the $[MeHg([12]aneS_3)]^+$ complex in crystals of **2** (hydrogen atoms are omitted); bond lengths [Å] and angles [°]: Hg−S1 2.441(4), Hg−C1 2.11(2), Hg···S2^{I} 3.176(4), Hg···S3^{II} 3.256(4), Hg···F1 2.97(1); S1−Hg−C1 168.1(6); symmetry transformations: ^{I}: 0.5 + *x*, 0.5 − *y*, 0.5 + *z*; ^{II}: 0.5 + *x*, 0.5 + *y*, *z*

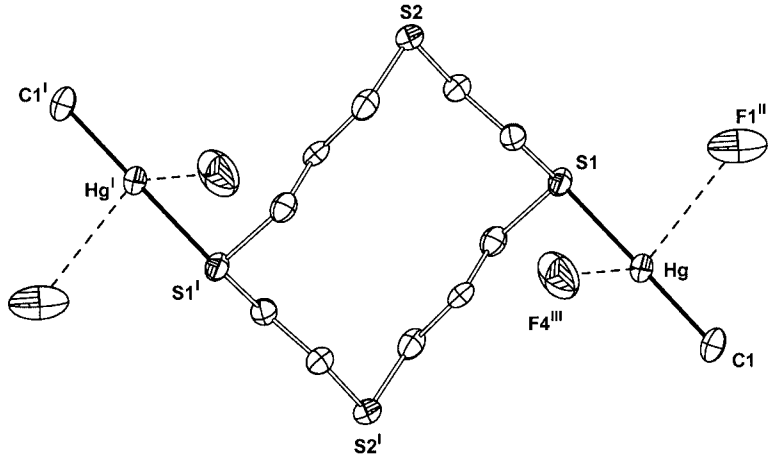

Figure 3. Ellipsoid plot (50% probability level) of the $[(MeHg)_2([14]aneS_4)]^{2+}$ complex in crystals of **3** (hydrogen atoms are omitted); bond lengths [Å] and angles [°]: Hg−S1 2.425(2), Hg−C1 2.068(7), Hg···F1^{II} 2.947(5), Hg···F4^{III} 2.946(5); S1−Hg−C1 174.7(2); symmetry transformations: ^{I}: − *x*, 2 − *y*, 2 − *z*; ^{II}: −0.5 + *x*, 1.5 − *y*, −0.5 + *z*; ^{III}: 0.5 − *x*, 0.5 + *y*, 1.5 − *z*

Properties in Solution and Behavior Towards Competing Ligands

At room temperature, **1**−**3** showed rapid ligand exchange resulting in averaged NMR signals for coordinated and free thioether ligands. In suitable solvents, the $[MeHg([9]aneS_3)]^+$ complex of **1** is rather stable against solvolysis. This was demonstrated by an NMR experiment in which increasing amounts of $[MeHg(OH_2)](BF_4)\cdot xH_2O$ were added to a 0.06 M solution of $[9]aneS_3$ in CD_3CN. The $^2J(^1H,^{199}Hg)$ value was found to be independent of the $MeHg^+/[9]aneS_3$ molar ratio in the range of 0.5−0.95:1 and identical to the coupling constant measured for solutions of **1** in CD_3CN. At ratios > 1:1, the carbon atoms of the thioether showed a constant chemical shift identical to that observed for **1**. The two NMR quantities $^2J(^1H,^{199}Hg)$ and $\delta_C(CH_2)$ differ clearly between **1** (237.4 Hz; 30.4 ppm) and the "free" components ($[MeHg(OH_2)]^+$: ca. 260 Hz; $[9]aneS_3$: 35.4 ppm). A marked dissociation equilibrium would be sensitive to an excess of either of the two starting materials, resulting in non-constant values of the NMR parameters. The experimental results thus enabled us to conclude that $[MeHg([9]aneS_3)]^+$ does not strongly dissociate in CD_3CN.

An analogous experiment with $[12]aneS_3$ showed that the $[MeHg([12]aneS_3)]^+$ complex in **2** is markedly dissociated in CD_3CN. At a $MeHg^+/[12]aneS_3$ molar ratio of 0.5:1 the $^2J(^1H,^{199}Hg)$ coupling constant was 221.9 Hz (**2**: 224.2 Hz), indicating a more complete complexation of methylmercury due to the excess of thioether. When the ratio was increased from 1:1 to 4.5:1, a continuous increase in the $^2J(^1H,^{199}Hg)$ value resulted. However, this increase was significantly smaller than expected from the contribution of $[MeHg(OH_2)]^+$ or $[MeHg(NCCD_3)]^+$. This discrepancy can be explained by the binding of more than one methylmercury group per thioether molecule. From the $\delta_C(MeHg)$ values {8.9 ppm at $MeHg^+/[12]aneS_3$ = 1:1; 4.5 ppm at 4.5:1; $[MeHg(OH_2)]^+$: ca. 0.0 ppm} one can easily estimate that at the highest $MeHg^+/[12]aneS_3$ ratio (4.5:1) each thioether ligand binds, on average, slightly more than two $MeHg^+$ cations. Consistent with this picture, the $\delta_C(SCH_2)$ value of the ligand continuously increased from 30.3 ppm (at 1:1) to 32.6 ppm (at 4.5:1). The value for free $[12]aneS_3$ is 28.9 ppm.

Some years ago, Rabenstein suggested that the $^2J(^1H,^{199}Hg)$ coupling constant of the methylmercury group may be utilized as a general indicator of the presence of chelating ligands.[48] Indeed, it has been reported that complexes of potentially chelating ligands of the 2,2′-bipyridyl and 1,10-phenanthroline type have higher values (235.1−239.8 Hz) than those of monodentate pyridine derivatives (225.2−229.6 Hz).[49] A comparison of $[MeHg\{N(CH_2CH_2PPh_2)_3\}]^+$ (174 Hz, CN 4)[28] with $[MeHg(PR_3)]^+$ complexes (167−173 Hz, CN 2)[50] shows the same trend, albeit less pronounced. Accordingly, we observed a higher ^2J value for the tetrahedral complex $[MeHg([9]aneS_3)]^+$ (237.4 Hz) than for the two-coordinate $[MeHg([12]aneS_3)]^+$ species (224.2 Hz). The latter value compares well with coupling constants found for other two-coordinate thioether complexes, e.g. $[MeHg(SMe_2)]^+$ (220.7 Hz),[35b] [MeHg(methionineH)]$^{2+}$ (223 Hz),[32] and $[MeHg(SEt_2)]^+$ (218 Hz; see Exp. Sect.). Surprisingly, $[(MeHg)_2([14]aneS_4)]^{2+}$, which exhibits primary two-coordination in crystals of **3** (see above), has a relatively large coupling constant (231.1 Hz) which is strongly temperature-dependent. Raising the temperature from −30 to +60 °C resulted in an increase by 9.7 Hz (**1**: 1.9 Hz; **2**: 2.6 Hz). One possible explanation is that **3** is more strongly dissociated than, for example, **2**. In this case, the contribution of the dissociation product $[MeHg(NCCD_3)]^+$ would increase the observed (average) ^2J value. Another explanation is supported by the observation that the Hg−C bonds are activated towards protonolytic cleavage in $[(MeHg)_2([14]aneS_4)]^{2+}$ but not in $[MeHg(SEt_2)]^+$ (see below). It is conceivable that in solution, three-coordinate isomers of the former complex exist where the $[14]aneS_4$ ligand forms five-membered HgS_2C_2 chelate rings. This binding situation has a precedent in the complex $[(HgCl_2)_2([14]aneS_4)]$, in which the thioether is simultaneously coordinated to two $HgCl_2$ moieties.[51] Higher temperatures may favor the accompanying ligand conformations which are probably energetically less favored than the one observed in crystalline **3**.

The ^1H NMR spectrum of **1** at −30 °C shows that the tetrahedral structure observed in the solid state is retained in solution. The signal of the CH_2 groups forms a characteristic AA′BB′ (or AA′XX′) pattern[52] in accordance with the presence of three five-membered chelate rings which rapidly alternate between the λ and δ conformations (Scheme 1).

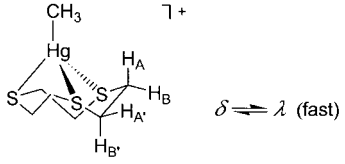

Scheme 1

Upon raising the temperature, this pattern collapses into a broad and finally, at 60 °C, a sharp singlet, obviously because of fast exchange of the thioether ligand. Between −30 °C and room temperature, $^2J(^1H,^{199}Hg)$ (see above) and the coordination-induced chemical shifts of **1** are practically temperature-independent. For example, the relative shift of the CH_2 groups $\Delta\delta_C = \delta_C(\text{coordinated}) - \delta_C(\text{free ligand})$ has a constant value of −5.0 ppm in CD_3CN. It can therefore be concluded that the tetrahedral structure is also present at room temperature. In the room temperature ^1H and ^{13}C NMR spectra of **2** and **3**, the number of observed resonances is less than would be expected from the solid-state structures. This can be explained either by fast thioether ligand exchange as in the case of **1**, fast intramolecular migration of the $MeHg^+$ group(s) at the macrocycle via intermediate chelates, or both. At −30 °C, the number and multiplicity of the signals remain unchanged. Thus, at this

temperature, at least one of these processes cannot be "frozen" as opposed to the ligand exchange in **1**.

The relative stability of $[MeHg([9]aneS_3)]^+$ towards a number of neutral or monoanionic potential ligands, $L^{(-)}$, was studied by NMR spectroscopy. In this study, fast ligand exchange at room temperature proved beneficial because it resulted in only one ^{13}C NMR signal for mixtures of coordinated and released $[9]aneS_3$. The position of this signal between the two extremes, δ_C(coordinated) = 29.5 ppm and δ_C(free ligand) = 33.9 ppm, gave a qualitative indication of the position of equilibrium [Equation (2)].

$$[MeHg([9]aneS_3)]^+ + L^{(-)} \leftrightarrows [MeHgL]^{(+)} + [9]aneS_3 \quad (2)$$

The δ_C values are given for solutions in $[D_6]$DMSO, which was used for solubility reasons. The solutions were initially 50 mM in each of the two components **1** and $L^{(-)}$. L^- anions were introduced as their Et_4N^+ salts. It appeared that the position of the equilibrium according to Equation (2) was far to the left side when L^- was an oxo anion with a largely delocalized charge such as $CF_3SO_3^-$, *p*-$CH_3C_6H_4SO_3^-$ or NO_3^-. With $L^{(-)} = CH_3CO_2^-$, F^-, Cl^-, Br^-, I^- or PPh_3, however, complete substitution of the thioether ligand was observed. An intermediate situation occurred with $L^{(-)} = CF_3CO_2^-$ or NEt_3 where the equilibrium concentrations of $[MeHg([9]aneS_3)]^+$ and $[MeHgL]^{(+)}$ were of the same order of magnitude. As expected, the monodentate ligand $[12]aneS_3$ cannot displace the tridentate $[9]aneS_3$ (experiment conducted in CD_3CN). In summary, it can be concluded that $[9]aneS_3$ is an unusually strong ligand for $MeHg^+$ when compared with other thioethers, but still a rather weak ligand on an absolute scale, comparable for example with trifluoroacetate.

Hypothetical Reaction Mechanism of Organomercurial Lyase

The bacterial enzyme organomercurial lyase catalyzes the simple reaction shown in Equation (3) (R = alkyl, aryl). A model for the reaction mechanism of this enzyme was proposed some years ago[20,27] (see Introduction) and has very recently been refined.[53] It consists of at least four steps (Scheme 2).

$$RHg^+ + H^+ \rightarrow Hg^{2+} + RH \quad (3)$$

Step 1: Enz(-SH)$_2$ + RHg(SR') ⇌ HS-Enz-SHgR + R'SH

Step 2: HS-Enz-SHgR ⟶ Enz-S$_2$Hg + RH

Step 3: Enz-S$_2$Hg + R'SH ⇌ HS-Enz-SHg(SR')

Step 4: HS-Enz-SHg(SR') + R'SH ⇌ Enz(-SH)$_2$ + Hg(SR')$_2$

Scheme 2. Reaction steps in the mechanism of organomercurial lyase (Enz = enzyme)

In the first step, a cysteinyl-SH group of the enzyme protonates and displaces an exogenous thiolate, such as the anion of cysteine or glutathione (R′SH), thereby binding the RHg^+ cation at the active site. There the key step follows, namely the protonolytic Hg−C bond cleavage, in which a second SH group of the enzyme is involved (step 2). In the last two steps, exogenous thiolates coordinate to the product Hg^{2+} and finally remove it from the enzyme. Pitts and Summers proposed that Cys159[54] could be the primary ligand for the substrate RHg^+ (step 1), while Cys96 donates the proton in step 2.[53] They also pointed out that further amino acid residues, for example Tyr93 and Cys117, are possible candidates as ligands and/or proton donors. The latter is also one of three highly conserved cysteines, besides Cys96 and Cys159. However, there are indications that Cys117 may have no catalytic function.

From the viewpoint of coordination chemistry, step 2 is the most intriguing one. It raises the question of how the Hg−C bond is activated for protonolysis. From model studies on phosphane[28] and thioether complexes (this work), it seems less likely that sufficient activation of the Hg−C bond is possible in the binding situation depicted in Scheme 3 (A). Here, Cys96 can only act as a weak thiol donor and has a spatial orientation typical of secondary ligands. Scheme 3 (B) shows the original proposal[20,27] extended by recent biochemical results.[53] The mercury atom is three-coordinate, and therefore an enhanced polarity and a significant activation of the Hg−C bond may be expected. In Scheme 3 (C) we suggest a model that carries features of both previous ones and takes into account the occurrence of several conserved OH-containing amino acid residues in the enzymes. In this model, activation and protonation depend on the participation of Y−OH, which represents an alcoholic or a phenolic amino acid residue. Alternatively Y−OH could be a water molecule, which may be involved in hydrogen bonding to an OH-containing side chain. The oxygen atom of Y−OH simultaneously serves as proton acceptor (from Cys96−SH) and donor (to R^-). Proton withdrawal from Cys96−SH imposes thiolate character on the sulfur atom. This, together with the overall spatial arrangement, would allow the formation of a second primary Hg−S bond. Candidates for Y−OH include the conserved residues Thr77, Thr81, Tyr93, Ser115, and Thr120. In addition, the ligand AA−X^- (shown in Scheme 3, B) could also be present here. The model in Scheme 3 (C) is purely hypothetical but it is supported by results of quantum chemical calculations, which are presented below. It might be tested experimentally on suitable site-directed mutants.

Protonolysis of Hg−C Bonds in Methylmercury Thioether Complexes

The four-coordinate complex $[MeHg([9]aneS_3)]^+$ offered the opportunity of studying, for the first time, the effect of multiple sulfur ligation on the reactivity of the Hg−C bond. The very strong Brønsted acid CF_3SO_3H in $[D_3]$nitromethane was used as proton donor.[55] An additional equivalent of $[9]aneS_3$ was employed in order to trap the reaction product Hg^{2+} as $[Hg([9]aneS_3)_2]^{2+}$. After the protonolysis step, the thioether is thus functionally similar to the exogenous thiols in the mechanism of organomercurial lyase

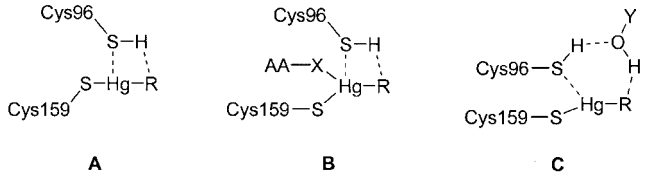

Scheme 3. Proposals for the key step of the reaction mechanism of organomercurial lyase; A: with only Cys96 and Cys159 being involved; B: with a further primary ligand $AA-X^-$, for example Tyr93 (X = O) or Cys117 (X = S); C: with participation of an additional amino acid (or water) Y–OH as a simultaneous proton donor and acceptor

(steps 3 and 4). The overall reaction can be expressed by Equation (4).

$$[MeHg([9]aneS_3)]^+ + CF_3SO_3H + [9]aneS_3 \rightarrow [Hg([9]aneS_3)_2]^{2+} + CF_3SO_3^- + CH_4 \quad (4)$$

Methane was identified as one of the reaction products by using deuterated acid. In the CF_3SO_3D-containing system, a mixture of CH_3D and CH_4 formed due to the presence of traces of H_2O (see below). For CH_3D we measured $^2J(H,D) = 1.9$ Hz and a deuterium isotope effect $\delta_H(CH_3D) - \delta_H(CH_4) = -15.3$ ppb in [D$_3$]nitromethane. These results are in good agreement with very accurately measured values in different solvents, for example in [D$_6$]-acetone: 1.9361 ± 0.0008 Hz and −15.555 ± 0.002 ppb.[56] The reaction product $[Hg([9]aneS_3)_2]^{2+}$ could be isolated as crystalline $[Hg([9]aneS_3)_2](BF_4)_2 \cdot 2\,CH_3CN$ (**4**) when the reaction was carried out in acetonitrile with HBF_4 instead of CF_3SO_3H [Equation (5)].

$$[MeHg([9]aneS_3)](BF_4) + HBF_4 + [9]aneS_3 \xrightarrow{CH_3CN} [Hg([9]aneS_3)_2](BF_4)_2 \cdot 2CH_3CN + CH_4 \quad (5)$$

Compound **4** was obtained in 72% yield. Its identity was confirmed by comparison with a sample that had been prepared independently from $HgPh_2$, HBF_4, and [9]aneS$_3$. Compound **4** was characterized, inter alia, by an X-ray structural analysis. In the crystals, the $[Hg([9]aneS_3)_2]^{2+}$ cation is located on a crystallographic center of inversion. The six sulfur atoms form a distorted octahedral coordination environment around the metal atom (see Figure 4). The molecular structure will not be further discussed here, since it is similar to those of other $[Hg([9]aneS_3)_2]^{2+}$ salts whose structures have already been described in the literature.[57]

The progress of the reaction according to Equation (4) was monitored by NMR spectroscopy, but attempts to determine kinetic data were unsuccessful because the measurements were impaired by unavoidable traces of water (ca. 0.3 equiv.). The effect of water could be demonstrated by intentionally adding 1 equiv., which almost entirely suppressed the protonolysis reaction. However, as the water content was the same in all experiments, it was possible to obtain semi-quantitative values to compare the relative reactivities of different $MeHg^+$ complexes. We found for example, that under the conditions described in the Exp. Sect., the degree of protonolysis reached ca. 25% for both **1** and **3** after 1 h. In contrast, $[MeHg(SEt_2)]^+$ and MeHgCl showed no detectable reaction even after 24 h. MeHgCl is known to be resistant towards strong acids; concentrated hydrochloric acid, for example, causes less than 1% protonolysis after 100 min.[58] This is despite the fact that chloride forms a stronger 1:1 $MeHg^+$ complex than [9]aneS$_3$, as our competition experiments have shown (see above). It therefore seems very likely that the higher coordination number in $[MeHg([9]aneS_3)]^+$ compared with MeHgCl is the most crucial factor in Hg–C bond activation. The large difference in reactivity between $[(MeHg)_2([14]aneS_4)]^{2+}$, which is two-coordinate in crystals of **3**, and $[MeHg(SEt_2)]^+$ appears to contradict this conjecture. However, the $^2J(^1H,^{199}Hg)$ value indicates that in solutions of **3**, the coordination number of mercury may exceed 2, as already discussed. In order to better understand the role of the coordination number, quantum chemical calculations were carried out.

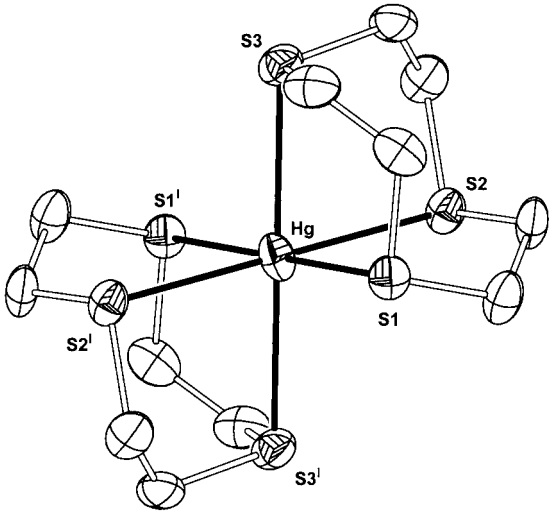

Figure 4. Ellipsoid plot (50% probability level) of the $[Hg([9]aneS_3)_2]^{2+}$ complex in crystals of **4** (hydrogen atoms are omitted); bond lengths [Å] and angles [°]: Hg–S1 2.677(1), Hg–S2 2.660(1), Hg–S3 2.711(1); S1–Hg–S2 83.69(3), S1–Hg–S3 82.49(3), S1–Hg–S1^I 180.0, S1–Hg–S2^I 96.31(3), S1–Hg–S3^I 97.51(3), S2–Hg–S3 83.14(3), S2–Hg–S2^I 180.0, S2–Hg–S3^I 96.86(3), S3–Hg–S3^I 180.0; symmetry transformation: ^{I}: $-x, 1-y, -z$

Results of Quantum Chemical Calculations

In the following, structural properties[59] such as metrical data as well as NMR chemical shifts and mechanistic pathways for Hg–C bond activation[60] have been examined. In order to obtain reliable data, for example on coordination-induced chemical shifts, it is of the utmost importance to find a method/basis set combination that allows the accurate description of the molecules studied herein. In a first attempt, we therefore employed several ab initio and density functional theoretical approaches to reproduce the structure of the $[MeHg([9]aneS_3)]^+$ cation of **1**, the main focus

Table 1. Metal−ligand bond lengths [Å] in the complex $[MeHg([9]aneS_3)]^+$, determined at different levels of theory, compared with the experimental values

Method	Hg−C	Hg−S
X-ray diffraction	2.075(8), 2.080(8)	2.611(2)−2.768(2) (mean: 2.711)
AM1	2.057	2.738−2.752
PM3	2.076	2.590
B3LYP/LANL2DZ	2.237	2.986−2.997
B3LYP/SDD + SDD ECP Hg	2.143	2.886−2.912
B3LYP/SDD + SDD ECP Hg, 6-31G(d) C,H,S	2.138	2.856−2.864
BP86/SDD + SDD ECP Hg, 6-31G(d) C,H,S	2.134	2.839−2.844
B3LYP/SDD + SDD ECP Hg, SDD + 6-31G(d) C,H,S	2.137	2.858−2.870
B3LYP/SDD + SDD ECP Hg, SDD + 6-31+G(d,p) C,H,S	2.136	2.856−2.866
MP2/SDD + SDD ECP Hg, 6-31G(d) C,H,S	2.110	2.771−2.776
MP2/SDD + SDD ECP Hg, 6-31+G(d,p) C,H,S [a]	2.111	2.768−2.774

[a] In the discussion this level of theory is denoted MP2/I.

being on the Hg−C and Hg−S bond lengths. Table 1 summarizes the results. In each case, the basic structural feature of the complex, i.e. the tetrahedral coordination of mercury, is reproduced. The necessity of including a large basis set as well as an effective core potential can be clearly seen from the DFT calculations.[61] However, the Hg−S bonds were still much too long. Only the treatment at the correlated level[62] gave good agreement for these distances. Therefore the last method from Table 1 was used for the subsequent NMR calculation. Interestingly, the bond lengths were also well reproduced by the AM1 method. However, despite the good semiempirical description of the experimental structure, all evaluated ab initio calculations of NMR chemical shifts based on both AM1 and PM3 geometries failed to give satisfactory results.

As mentioned before, a reliable structure is indispensable for the evaluation of NMR chemical shifts in general,[63] and for organomercury compounds in particular.[64] The approach used herein applied the MP2-GIAO method[65] together with the SDD basis set and an ECP on mercury,[66] and the 6-31+G(d,p) basis set[67] on the remaining atoms based on the MP2-optimized geometries of $[MeHg([9]aneS_3)]^+$ and $[9]aneS_3$. Experimentally, a coordination-induced shift of −5.0 ppm (from 35.4 to 30.4 ppm) was observed for the CH_2 carbon atoms of the thioether ligand (see above). Such a high-field shift is perhaps counter-intuitive. However, it was reproduced quite accurately by our theoretical model: the averaged ^{13}C NMR shift changed by −7.4 ppm (from 38.9 to 31.5 ppm) when $[9]aneS_3$ underwent coordination. The ^{13}C NMR signal position of the methanido ligand of $[MeHg([9]aneS_3)]^+$, which has been found experimentally at 0.7 ppm, was also satisfactorily reproduced by theory (at $\delta = -3.1$ ppm).

The protonolytic cleavage of $Hg-CH_3$ bonds by trifluoromethanesulfonic acid has been investigated at several levels of theory (for pertinent experimental results see above). This includes the transition state for the proton transfer from CF_3SO_3H to methylmercury complexes of the type $[MeHgL]^{+\text{ or }0}$ leading to methane and, initially,

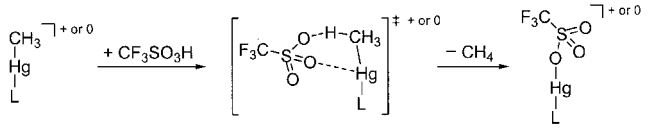

Scheme 4. Pathway of the reaction between $[MeHgL]^{+\text{ or }0}$ and trifluoromethanesulfonic acid (L = Cl^-, SEt_2, $MeSCH_2CH_2SMe$, or $[9]aneS_3$)

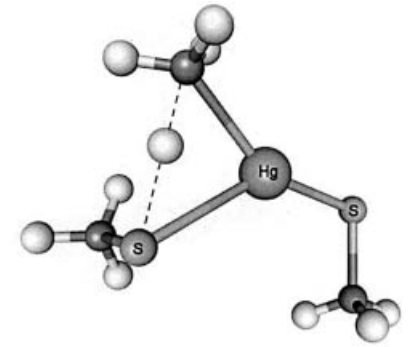

TS1

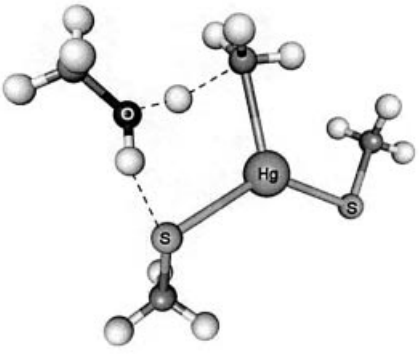

TS2

Figure 5. MP2/I-calculated transition states for the protonolytic Hg−C bond cleavage in MeHg(SMe) by methanethiol with (TS2), and without (TS1) assistance by methanol

$[(CF_3SO_3)HgL]^{+\text{ or }0}$ (Scheme 4). The latter can further react with another L to yield $[HgL_2]^{2+\text{ or }0}$.

The results of the MP2/I calculations (see Table 1 for basis set explanation) show that the hydrogen transfer activation barriers for the two complexes with digonal mercury coordination are similar, namely 23 kcal·mol^{-1} for MeHgCl and 20 kcal·mol^{-1} for $[MeHg(SEt_2)]^+$. Significantly lower activation barriers were found for the complexes with higher coordination numbers of mercury: 14 kcal·mol^{-1} for $[MeHg(MeSCH_2CH_2SMe)]^+$ (CN 3) and 12 kcal·mol^{-1} for $[MeHg([9]aneS_3)]^+$ (CN 4). This confirms the above described experimental finding that multiple sulfur ligation activates Hg−CH_3 bonds towards protonolytic cleavage. The possible relevance for the enzymatic reaction mechanism is obvious.

Finally, we sought an answer for the possible involvement of OH-containing amino acid residues in the enzymatic reaction mechanism. The model investigated consists of methylmercury methanethiolate i.e. MeHg(SMe), to which a proton is transferred from methanethiol, either directly or by assistance from methanol. Our model corresponds to the situations depicted in Scheme 3 (A and C). Optimization of the two proton transfer transition states at the MP2/I level of theory (Figure 5) demonstrates a clear preference of 14 kcal·mol^{-1} for the six-membered transition structure TS2 which involves the additional hydroxy group. The activation energies for the two pathways are 39 and 25 kcal·mol^{-1}, respectively. Although these values are still high for an enzymatic reaction this model shows, that the involvement of OH groups can significantly lower the activation barrier for protonolytic Hg−C bond cleavage, and should therefore be considered when discussing possible reaction mechanisms of organomercurial lyase.

Conclusions

The following are the principal results and conclusions of this work: (i) Complexes between the methylmercury(1+) cation and the cyclic thioethers [9]aneS_3, [12]aneS_3, and [14]aneS_4 are isolable as crystalline tetrafluoroborates $[MeHg([9]aneS_3)](BF_4)$ (**1**), $[MeHg([12]aneS_3)](BF_4)$ (**2**), and $[(MeHg)_2([14]aneS_4)](BF_4)_2$ (**3**), respectively, in good yields. In **2** and **3**, Hg^{II} has an unexceptional linear coordination. In **1**, however, the thioether acts as a tridentate ligand. The resultant tetrahedral metal coordination is rarely found in organomercury compounds. (ii) The unusual coordination has a distinct influence on the reactivity of $[MeHg([9]aneS_3)]^+$. This complex is significantly more stable to substitution of its sulfur ligand than other $MeHg^+$−thioether complexes. Besides, its Hg−C bond is much more susceptible to cleavage by a strong Brønsted acid than the Hg−C bonds in linear coordinated $[MeHg(SEt_2)]^+$ or MeHgCl. Quantum chemical calculations confirm that the coordination number is an important factor in Hg−C bond activation. (iii) Our experimental and theoretical findings strengthen the hypothesis that multiple sulfur coordination, in this case by cysteinyl S atoms, plays a key role in the mechanism of organomercurial lyase. Assistance by an OH group, for example from an amino acid side chain, could further facilitate the protonolytic Hg−C bond cleavage in the enzyme's active site.

Experimental Section

Safety Precautions: Soluble mercury(II) compounds are highly toxic. In addition to the precautions routinely taken when toxic metal species are handled, further protection measures are necessary when working with methylmercury ($MeHg^+$).[10,11,68] In particular, laminate gloves that are specially designed for chemical resistance (Silver Shield) should be worn under neoprene or nitrile gloves. Disposable latex gloves are not sufficient! Medical surveillance of the mercury concentration in the blood should be considered for those repeatedly working with methylmercury compounds. Methylmercury-containing wastes can be treated with strong oxidants, for example aqua regia, to give inorganic mercury (Hg^{2+}). Using the "supertoxic" compound dimethylmercury as an Hg NMR standard is not to be recommended (see below).

Instrumentation: ^1H and $^{13}C\{^1H\}$ NMR spectra were recorded at 300 K with a Bruker DPX 300 or a DRX 500 instrument. Chemical shifts are given relative to TMS (δ = 0 ppm). $^{199}Hg\{^1H\}$ NMR spectra were recorded with the DRX 500 spectrometer at 290 K. A 0.10 M solution of $Hg(ClO_4)_2$ in 0.10 M perchloric acid in D_2O served as an external standard.[69,70] The standard was prepared as follows: in a 1-mL volumetric flask, D_2O was added to yellow HgO (21.7 mg, 0.100 mmol) and $DClO_4$ (26.4 μL of a 68% solution in D_2O, ρ = 1.694 g·cm^{-3}, 0.300 mmol); after ca. 30 min, the HgO had completely dissolved, and the flask was filled to the mark. ^{199}Hg chemical shifts were referenced to neat $HgMe_2$ (δ_{Hg} = 0 ppm) with this solution (δ_{Hg} = −2250 ppm on the $HgMe_2$ scale). IR spectra (KBr pellets) were obtained with a Bio-Rad FTS 7PC spectrometer. Mass spectra were measured with a Finnigan MAT 212 instrument. Melting points were determined in unsealed glass capillaries. Elemental analyses were performed by the Mikroanalytisches Labor Pascher, Remagen (Germany).

Starting Materials: The ligand 1,5,9-trithiacyclododecane ([12]aneS_3) was prepared according to a literature method starting from bis(3-hydroxypropyl) sulfide.[45] The other starting materials, including methylmercury hydroxide (1 M aqueous solution, Alfa Aesar), were purchased from commercial sources and used as received. The solvents were of reagent grade.

Preparation of $[MeHg([9]aneS_3)](BF_4)$ (1): HBF_4 (150 μL of a 50% aqueous solution, ρ = 1.38 g·cm^{-3}, 1.2 mmol) was added to MeHgOH (1.00 mL of a 1 M aqueous solution, 1.0 mmol). After 12 h, the solution was concentrated in vacuo to give a colorless oil, which was redissolved in tetrahydrofuran (2 mL). A solution of [9]aneS_3 (180 mg, 1.00 mmol) in tetrahydrofuran (5 mL) was added dropwise whilst stirring. A white, microcrystalline solid formed immediately. After stirring for 12 h, the reaction was complete, and the solid was collected on a glass filter, washed with tetrahydrofuran and dried under vacuum. Yield: 412 mg (85%). M.p. ca. 190 °C (dec.). ^1H NMR (300 MHz, CD_3CN, 40 mM): δ = 1.09 [s with satellites, $^2J(^1H,^{199}Hg)$ = 237.4 Hz, 3 H; $HgCH_3$], 3.09 (br. s, 12 H, CH_2) ppm. ^{13}C NMR (75.5 MHz, CD_3CN, 40 mM): δ = 0.7 ($HgCH_3$, superposed by solvent signal[71]), 30.4 (CH_2) ppm. ^{199}Hg NMR (89.6 MHz, CD_3CN, 40 mM): δ = −194 ppm. IR: $\tilde{\nu}$ = 2920 (w), 1449 (m), 1410 (m), 1287 (m), 1161 (w), 1144 (w), 1047 (s, br), 1036 (s, br), 926 (m), 889 (m), 816 (m), 783 (m), 521 cm^{-1} (m). MS

(CI, isobutane): *m/z* (%) = 397 (2) $[MeHg([9]aneS_3)]^+$, 181 (100) $[[9]aneS_3 + H]^+$. $C_7H_{15}BF_4HgS_3$ (482.8): calcd. C 17.41, H 3.13, Hg 41.55, S 19.93; found C 17.35, H 3.03, Hg 41.2, S 19.8.

Preparation of $[MeHg([12]aneS_3)](BF_4)$ (2): HBF_4 (75 μL of a 50% aqueous solution, ρ = 1.38 g·cm^{-3}, 0.6 mmol) was added to MeHgOH (0.50 mL of a 1 M aqueous solution, 0.5 mmol). After 12 h, the solution was concentrated in vacuo to give a colorless oil, to which $[12]aneS_3$ (111 mg, 0.50 mmol), dissolved in acetonitrile (5 mL), was added. The reaction flask was connected to another flask that contained diethyl ether. During the next 7 d the diethyl ether was allowed to diffuse into the reaction mixture through the gas phase. A colorless, crystalline solid formed, which was collected on a glass filter, washed with tetrahydrofuran and dried under vacuum. Yield: 179 mg (68%). M.p. ca. 166 °C (dec.). ^{1}H NMR (300 MHz, CD_3CN): δ = 1.11 [s with satellites, $^2J(^1H,^{199}Hg)$ = 224.2 Hz, 3 H, $HgCH_3$], 1.99 (quint, $^3J_{H,H}$ = 6.6 Hz, 6 H, $CH_2CH_2CH_2$), 2.93 (t, $^3J_{H,H}$ = 6.6 Hz, 12 H, SCH_2) ppm. ^{13}C NMR (75.5 MHz, CD_3CN): δ = 8.9 ($HgCH_3$), 27.0 ($CH_2CH_2CH_2$), 30.3 (SCH_2) ppm. ^{199}Hg NMR (89.6 MHz, CD_3CN, 40 mM): δ = −886 ppm. IR: ṽ = 2926 (w), 1449 (m), 1431 (m), 1416 (m), 1300 (w), 1260 (m), 1250 (m), 1177 (w), 1049 (s, br), 1030 (s, br), 793 (m), 756 (m), 519 cm^{-1} (m). MS (CI, isobutane): *m/z* (%) = 439 (4) $[MeHg([12]aneS_3)]^+$, 223 (100) $[[12]aneS_3 + H]^+$. $C_{10}H_{21}BF_4HgS_3$ (524.9): calcd. C 22.88, H 4.03, Hg 38.22, S 18.33; found C 22.88, H 3.90, Hg 38.4, S 18.3.

Preparation of $[(MeHg)_2([14]aneS_4)](BF_4)_2$ (3): HBF_4 (150 μL of a 50% aqueous solution, ρ = 1.38 g·cm^{-3}, 1.2 mmol) was added to MeHgOH (1.00 mL of a 1 M aqueous solution, 1.0 mmol). After 12 h, the solution was concentrated in vacuo to give a colorless oil, to which $[14]aneS_4$ (134 mg, 0.50 mmol), dissolved in acetonitrile (5 mL), was added. The reaction flask was connected to another flask that contained diethyl ether. During the next 4 d the diethyl ether was allowed to diffuse into the reaction mixture through the gas phase. Small, plate-like crystals formed, which were collected on a glass filter, washed with a small amount of tetrahydrofuran and dried under vacuum. Yield: 403 mg (92%). M.p. ca. 129 °C (dec.). ^{1}H NMR (500 MHz, CD_3CN): δ = 1.16 [s with satellites, $^2J(^1H,^{199}Hg)$ = 231.1 Hz, 6 H, $HgCH_3$], 2.10 (quint, $^3J_{H,H}$ = 7.3 Hz, 4 H, $CH_2CH_2CH_2$), 3.05 (t, $^3J_{H,H}$ = 7.3 Hz, 8 H, $CH_2CH_2CH_2$), 3.26 (s, 8 H, SCH_2CH_2S) ppm. ^{13}C NMR (125.8 MHz, CD_3CN): δ = 7.6 ($HgCH_3$), 30.2 ($CH_2CH_2CH_2$), 32.7 ($CH_2CH_2CH_2$), 33.3 (SCH_2CH_2S) ppm. IR: ṽ = 2942 (w, br), 1445 (m), 1287 (w), 1215 (w), 1182 (m), 1084 (s, br), 1051 (s, br), 1036 (s, br), 789 (m), 521 cm^{-1} (m). MS (CI, isobutane): *m/z* (%) = 485 (2) $[MeHg([14]aneS_4)]^+$, 351 (6) $[MeHg([7]aneS_2)]^+$,[72] 107 (100) $[C_3H_6S_2$ (dithiolane) + $H]^+$. $C_{12}H_{26}B_2F_8Hg_2S_4$ (873.4): calcd. C 16.50, H 3.00, Hg 45.93, S 14.69; found C 16.75, H 3.00, Hg 45.7, S 14.7.

Preparation of $[Hg([9]aneS_3)_2](BF_4)_2 \cdot 2\ CH_3CN$ (4). Method A: Diphenylmercury (177 mg, 0.50 mmol) and $[9]aneS_3$ (180 mg, 1.00 mmol) were dissolved in tetrahydrofuran (10 mL). Addition of HBF_4 (152 μL of a 54% solution in diethyl ether, ρ = 1.19 g·cm^{-3}, 1.1 mmol) resulted in the immediate precipitation of a white, microcrystalline solid. After 6 h, the solid was collected on a glass filter, washed with tetrahydrofuran and redissolved in acetonitrile (20 mL) in a flask, which then was connected to another flask containing diethyl ether. During the next 5 d the diethyl ether was allowed to diffuse into the solution through the gas phase. Colorless, elongated tabular crystals formed, which were collected on a glass filter, washed with tetrahydrofuran and briefly dried under vacuum. Yield: 358 mg (88%). M.p. ca. 189 °C (dec.). ^{1}H NMR (300 MHz, CD_3CN): δ = 1.96 (s, ca. 6 H, CH_3CN), 2.9−3.3 (m, 24 H, SCH_2) ppm. ^{13}C NMR (75.5 MHz, CD_3CN): δ = 28.3 (SCH_2) ppm. ^{199}Hg NMR (89.6 MHz, CD_3CN, 40 mM): δ = −305 ppm. IR: ṽ = 2911 (w), 2899 (w), 2249 (w), 1443 (m), 1408 (m), 1300 (sh), 1285 (m), 1059 (s, br), 1036 (s, br), 920 (m), 883 (m), 822 (m), 534 (m), 521 (m), 424 cm^{-1} (m). MS (CI, isobutane): *m/z* (%) = 181 (100) $[[9]aneS_3 + H]^+$, 121 (97) $[C_4H_8S_2$ (dithiane) + $H]^+$. $C_{16}H_{30}B_2F_8HgN_2S_6$ (817.0): calcd. C 23.52, H 3.70, Hg 24.55, N 3.43, S 23.55; found C 23.58, H 3.57, Hg 25.0, N 3.15, S 23.9. **Method B:** HBF_4 (136 μL of a 54% solution in diethyl ether, ρ = 1.19 g·cm^{-3}, 1.0 mmol) was added whilst stirring to a solution of **1** (96 mg, 0.20 mmol) and $[9]aneS_3$ (36 mg, 0.20 mmol) in acetonitrile (5 mL). After stirring for ca. 30 min, the reaction mixture was stored at ca. 0 °C. After 24 h, colorless crystals of **4** had formed, which were collected on a glass filter, washed with a small amount of an ice-cold acetonitrile/diethyl ether mixture (1:1, v/v) and briefly dried under vacuum. Yield: 117 mg (72%). The ^{1}H and ^{13}C NMR spectra and the IR spectrum were identical to those of the material prepared by Method A.

Estimation of the Rates of Protonolysis: Solutions for the NMR measurements were prepared in a stream of dry nitrogen as a protection against atmospheric moisture. A typical experiment was conducted as follows. **1** (48.3 mg, 100 μmol) and $[9]aneS_3$ (18.0 mg, 100 μmol) were weighed out in a 1-mL volumetric flask, which had been flushed with dry nitrogen. Hexamethylbenzene (300 μL of a 50 mM stock solution in $[D_3]$nitromethane, 15.0 μmol) was then added, which served as a reference standard for determining the concentration change of methylmercury. After addition of $[D_3]$nitromethane (ca. 0.3 mL), the flask was shaken until a clear solution was obtained. Trifluoromethanesulfonic acid (98 μL of a 1.02 M stock solution in $[D_3]$nitromethane, 100 μmol) was then added. After briefly shaking, the flask was filled to the mark with $[D_3]$nitromethane. After shaking again, most of the solution was immediately transferred to an NMR tube, which had been flushed with dry nitrogen. The tube was sealed with a standard cap and parafilm. The initial ^{1}H NMR spectrum was measured typically 8 min after addition of the acid. Subsequent spectra were recorded every 3 min during the first 30 min, and later at increasingly longer time intervals. The temperature was kept at 20 °C. NMR spectroscopic data were collected over a period of ca. 6 h. The ^{1}H NMR spectra were analyzed by measuring the change of the integral intensity of the $MeHg^+$ signal (at δ = 1.10 ppm) relative to the signal of hexamethylbenzene (at δ = 2.19 ppm). For **3**, MeHgCl, and $[MeHg(SEt_2)]^+$ the sample preparations and measuring conditions were similar to those described above. However, the concentrations were adjusted less rigorously, and much longer time intervals between successive measurements were chosen because the main purpose was to establish whether the reaction had occurred at all. Between measurements, the NMR samples were stored at 20 °C. In the case of **3** (0.04 M solution), two moles of trifluoromethanesulfonic acid per mole of complex were applied and no hexamethylbenzene was added. Instead, the intensity of the $CH_2CH_2CH_2$ ligand signal served as a reference. It occurred at δ ≈ 2.45 ppm and, later, split to give an additional signal at δ = 2.36 ppm, which was assigned to the product complex(es) that formed as a result of the protonolysis. The MeHgCl solution was 0.07 M, and contained a known concentration (0.02 M) of hexamethylbenzene. $[MeHg(SEt_2)]^+$ was prepared in situ. To this end, aqueous solutions of MeHgOH (0.30 mmol) and HBF_4 (0.36 mol) were mixed. After 1 h, the reaction solvents were evaporated in vacuo. The residue was dissolved in nitromethane (ca. 0.7 mL), and the resultant solution was concentrated again. This procedure was repeated four times in order to remove water and excess HBF_4. The residue was then dissolved in $[D_3]$nitromethane (1.0 mL). Addition of 1 equiv.

of diethyl sulfide resulted in a sharp decrease in the $^2J(^1H,^{199}Hg)$ coupling constant from 251 to 218 Hz, indicating the formation of $[MeHg(SEt_2)]^+$ {^{1}H NMR (300 MHz, [D$_3$]nitromethane): δ = 1.17 [s with satellites, $^2J(^1H,^{199}Hg)$ = 218 Hz, 3 H, $HgCH_3$], 1.55 (t, $^3J_{H,H}$ = 7.3 Hz, 6 H, CH_2CH_3), 3.49 (q, $^3J_{H,H}$ = 7.3 Hz, 4 H; SCH_2)}. Finally, 1 equiv. of trifluoromethanesulfonic acid was added. The intensity of the SCH_2 signal of the thioether served as a reference.

X-ray Crystallography: Crystal data and details of the data collections and structural refinements are summarized in Table 2. The crystals were embedded in perfluoropolyalkyl ether (viscosity 1600 cSt., m.p. −20 °C; ABCR, Karlsruhe, Germany) and placed into glass capillaries. The capillaries were sealed and transferred into the cold gas stream of a STOE IPDS area detector diffractometer. Mo-K_α radiation (λ = 0.71073 Å) was used for intensity data collection. The measuring temperature was 193 K. Numerical absorption corrections were applied to the data. The structures were solved by direct methods and refined on F^2 values. Anisotropic displacement parameters were refined for the non-hydrogen atoms, except for the C atom of the $MeHg^+$ group of compound **2**, which gave unreasonable values on anisotropic refinement. All hydrogen atoms were included in idealized positions by use of riding models. Programs used were those of the SHELX-97 software package[73] and DIAMOND for the graphical representations.[74] **1:** Single crystals were grown by diffusion of diethyl ether through the gas phase into a solution of **1** in acetonitrile. The four largest peaks in the final difference map are located at distances < 0.9 Å from the Hg atoms. The remaining difference peaks are smaller than 0.7 e·Å^{-3}. **2:** A method similar to that described above for this compound yielded suitable single-crystals. The structure was successfully refined in the non-centrosymmetric space group *Cc*. The absolute structure parameter was −0.05(2) for the final model. **3:** Suitable single crystals were obtained using a procedure similar to that described above for this compound, however with use of a 1:1 ratio of the starting materials $[MeHg(OH_2)](BF_4)\cdot xH_2O$ and [14]aneS$_4$. **4:** Suitable single crystals were obtained by slow diffusion of diethyl ether through the gas phase into a solution of $[PhHg([9]aneS_3)](BF_4)$ in acetonitrile. Under these conditions, symmetrization of the $PhHg^+$ compound to **4** and $HgPh_2$ occurred.[37a] The BF_4^- anion is disordered; its F atoms were refined on two positions with an occupancy ratio of 2:1. CCDC-207378 (**1**), -207379 (**2**), -207380 (**3**), and -207381 (**4**) contain the supplementary crystallographic data for this paper. These data can be obtained free of charge at www.ccdc.cam.ac.uk/conts/retrieving.html [or from the Cambridge Crystallographic Data Center, 12 Union Road, Cambridge CB2 1EZ, UK; Fax: (internat.) + 44-1223/336-033; Email: deposit@ccdc.cam.ac.uk].

Computational Methods: The semiempirical calculations (AM1[75] and PM3[76]) employed the program package MOPAC 2002,[77] while the ab initio and DFT calculations were performed with Gaussian 98.[78] With the exception of a single B3LYP/LANL2DZ[79] optimization, all calculations at the correlated MP2 or the DFT BP86,[80] and the hybrid functional B3LYP[81][82] levels of theory used the Stuttgart/Dresden SDD basis set and the effective core potential for Hg.[66] The remaining atoms were described with the 6-31G(d) or 6-31+G(d,p) basis sets.[67] In two cases the SDD basis sets were added to these Pople bases. Local minima and transition states were verified by determination of the number of imaginary frequencies. Details of the NMR chemical shift calculations are given in the Results and Discussion section.

Acknowledgments

We thank Prof. Anne O. Summers and Dr. Irene Wagner-Döbler for providing information about structural and mechanistic details of organomercurial lyase. We also thank Prof. Martin Kaupp for helpful discussions on the computation of chemical shifts in Hg-containing systems. Financial support from the Deutsche Forschungsgemeinschaft and generous allocation of computer time at

Table 2. Crystallographic data and details of the data collection and structure refinement for compounds **1**−**4**

	1	**2**	**3**	**4**
Empirical formula	$C_7H_{15}BF_4HgS_3$	$C_{10}H_{21}BF_4HgS_3$	$C_{12}H_{26}B_2F_8Hg_2S_4$	$C_{16}H_{30}B_2F_8HgN_2S_6$
M_r	482.8	524.9	873.4	817.0
Crystal system	monoclinic	monoclinic	monoclinic	orthorhombic
Space group	$P2_1/c$	*Cc*	$P2_1/n$	*Pbca*
a [Å]	7.7802(4)	10.306(1)	8.6904(6)	8.8396(3)
b [Å]	42.319(2)	12.449(1)	13.951(1)	21.463(1)
c [Å]	8.6996(5)	12.590(1)	9.8959(9)	15.137(1)
β [°]	109.098(6)	92.067(10)	102.86(1)	90
V [Å^3]	2706.7(2)	1614.2(2)	1169.7(2)	2871.9(3)
Z	8	4	2	4
$\rho_{calcd.}$ [g cm^{-3}]	2.369	2.160	2.480	1.890
μ(Mo-K_α) [mm^{-1}]	11.852	9.946	13.526	5.858
Crystal size [mm]	0.40 × 0.33 × 0.21	0.70 × 0.16 × 0.06	0.36 × 0.17 × 0.12	0.44 × 0.27 × 0.18
Exposures	259	139	136	200
Oscillation angle for each exposure [°]	0.7	1.4	1.4	1.0
$2\Theta_{max.}$ [°]	52.06	51.56	51.54	51.96
Completeness to $2\Theta_{max.}$ [%]	95.0	94.7	93.5	94.5
Reflections collected	19449	5868	8270	21248
Independent reflections (R_{int})	5087 (0.1899)	2872 (0.0891)	2095 (0.0651)	2662 (0.1139)
Data/restraints/parameters	5087/0/289	2872/2/167	2095/0/128	2662/0/197
*R*1 [$I > 2\sigma(I)$]	0.0448	0.0499	0.0258	0.0232
*wR*2 (all data)	0.0907	0.1323	0.0597	0.0553
Goodness-of-fit on F^2	0.983	1.024	0.940	0.922
Largest difference peak/hole [e·Å^{-3}]	+2.06/−2.35	+1.16/−1.53	+1.05/−0.84	+0.31/−0.53

HLRN, Hannover (Germany), and APAC, Canberra (Australia), are gratefully acknowledged.

[1] C. H. Lamborg, W. F. Fitzgerald, J. O'Donnell, T. Torgersen, *Geochim. Cosmochim. Acta* **2002**, *66*, 1105−1118.

[2] United States Environmental Protection Agency, *Mercury Study Report to Congress*, vol. 3 ("Fate and Transport of Mercury in the Environment") to be found under http://www.epa.gov/oar/mercury.html, **1997**.

[3] W. F. Fitzgerald, R. P. Mason, in *Metal Ions in Biological Systems*, vol. 34 (Eds.: A. Sigel, H. Sigel), Dekker, New York, **1997**, pp. 53−111.

[4] R. P. Mason, W. F. Fitzgerald, F. M. M. Morel, *Geochim. Cosmochim. Acta* **1994**, *58*, 3191−3198.

[5] J. O. Nriagu, *Nature* **1989**, *338*, 47−49.

[6] J. O. Nriagu, J. M. Pacyna, *Nature* **1988**, *333*, 134−139.

[7] R. A. Bodaly, V. L. St. Louis, M. J. Paterson, R. J. P. Fudge, B. D. Hall, D. M. Rosenberg, J. W. M. Rudd, in *Metal Ions in Biological Systems*, vol. 34 (Eds.: A. Sigel, H. Sigel), Dekker, New York, **1997**, pp. 259−287.

[8] A. Boudou, F. Ribeyre, in *Metal Ions in Biological Systems*, vol. 34 (Eds.: A. Sigel, H. Sigel), Dekker, New York, **1997**, pp. 289−319.

[9] Committee on the Toxicological Effects of Methylmercury, National Research Council, *Toxicological Effects of Methylmercury*, National Academy Press, Washington, DC, **2000**; also to be found under http://www.nap.edu/books/0309071402/html/.

[10] D. W. Nierenberg, R. E. Nordgren, M. B. Chang, R. W. Siegler, M. B. Blayney, F. Hochberg, T. Y. Toribara, E. Cernichiari, T. Clarkson, *New Engl. J. Med.* **1998**, *338*, 1672−1676.

[11] H. Strasdeit, *Nachr. Chem. Tech. Lab.* **1998**, *46*, 846−848.

[12] United States Environmental Protection Agency, *Mercury Study Report to Congress*, vol. 5 ("Health Effects of Mercury and Mercury Compounds"), to be found under http://www.epa.gov/oar/mercury.html, **1997**.

[13] N. K. Mottet, M. E. Vahter, J. S. Charleston, L. T. Friberg, in *Metal Ions in Biological Systems*, vol. 34 (Eds.: A. Sigel, H. Sigel), Dekker, New York, **1997**, pp. 371−403.

[14] R. Hamada, K. Arimura, M. Osame, in *Metal Ions in Biological Systems*, vol. 34 (Eds.: A. Sigel, H. Sigel), Dekker, New York, **1997**, pp. 405−420.

[15] R. Hamada, M. Osame, in *Toxicology of Metals* (Ed.: L. W. Chang), CRC, Boca Raton, FL, **1996**, pp. 337−351.

[16] *The Toxicity of Methyl Mercury* (Eds.: C. U. Eccles, Z. Annau), Johns Hopkins University Press, Baltimore, **1987**.

[17] M. Schrope, *Nature* **2001**, *409*, 124.

[18] H. Strasdeit, A. von Döllen, W. Saak, M. Wilhelm, *Angew. Chem.* **2000**, *112*, 803−805; *Angew. Chem. Int. Ed.* **2000**, *39*, 784−786.

[19] L. Magos, in *Metal Ions in Biological Systems*, vol. 34 (Eds.: A. Sigel, H. Sigel), Dekker, New York, **1997**, p. 327.

[20] M. J. Moore, M. D. Distefano, L. D. Zydowsky, R. T. Cummings, C. T. Walsh, *Acc. Chem. Res.* **1990**, *23*, 301−308.

[21] In the absence of organomercurial lyase, mercury resistance is restricted to Hg^{2+} ("narrow-spectrum" resistance).

[22] S. M. Miller, in *Essays in Biochemistry*, vol. 34 (Ed.: D. P. Ballou), Portland Press, London, **1999**, pp. 17−30.

[23] A. M. Osborn, K. D. Bruce, P. Strike, D. A. Ritchie, *FEMS Microbiol. Rev.* **1997**, *19*, 239−262.

[24] J. L. Hobman, N. L. Brown, in *Metal Ions in Biological Systems*, vol. 34 (Eds.: A. Sigel, H. Sigel), Dekker, New York, **1997**, pp. 527−568.

[25] A. O. Summers, *Annu. Rev. Microbiol.* **1986**, *40*, 607−634.

[26] Transgenic plants engineered to express *merB* seem promising for the degradation of methylmercury at polluted sites; see for example: [26a] S. P. Bizily, C. L. Rugh, R. B. Meagher, *Nat. Biotechnol.* **2000**, *18*, 213−217. [26b] S. P. Bizily, C. L. Rugh, A. O. Summers, R. B. Meagher, *Proc. Natl. Acad. Sci. USA* **1999**, *96*, 6808−6813.

[27] T. P. Begley, A. E. Walts, C. T. Walsh, *Biochemistry* **1986**, *25*, 7192−7200.

[28] P. Barbaro, F. Cecconi, C. A. Ghilardi, S. Midollini, A. Orlandini, A. Vacca, *Inorg. Chem.* **1994**, *33*, 6163−6170.

[29] Tetrahedral coordination is very rare in organomercury chemistry. Instead, RHg^+ cations strongly prefer linear coordination of the Hg atom. Additional coordinate bonds occur frequently, but usually they are weak, "secondary" bonds: [29a] J. S. Casas, M. S. García-Tasende, J. Sordo, *Coord. Chem. Rev.* **1999**, *193−195*, 283−359. [29b] C. E. Holloway, M. Melník, *J. Organomet. Chem.* **1995**, *495*, 1−31.

[30] V. Barone, A. Bencini, F. Totti, M. G. Uytterhoeven, *J. Phys. Chem.* **1995**, *99*, 12743−12750.

[31] R. D. Bach, H. B. Vardhan, *J. Org. Chem.* **1986**, *51*, 1609−1610.

[32] M. T. Fairhurst, D. L. Rabenstein, *Inorg. Chem.* **1975**, *14*, 1413−1415.

[33] T. E. Jones, L. S. W. L. Sokol, D. B. Rorabacher, M. D. Glick, *J. Chem. Soc., Chem. Commun.* **1979**, 140−141.

[34] R. G. Pearson, *Inorg. Chem.* **1973**, *12*, 712−713.

[35] See for example: [35a] V. A. Nikanorov, V. I. Rozenberg, G. V. Gavrilova, O. A. Reutov, *Dokl. Akad. Nauk SSSR* **1982**, *262*, 108−113; English translation: *Dokl. Chem.* **1982**, *262*, 4−7. [35b] P. L. Goggin, R. J. Goodfellow, S. R. Haddock, J. G. Eary, *J. Chem. Soc., Dalton Trans.* **1972**, 647−653.

[36] [36a] *Cambridge Structural Database (CSD)*, version 5.24 (November 2002, 272066 entries) and updates (February−July 2003, 24361 entries). [36b] F. H. Allen, *Acta Crystallogr., Sect. B* **2002**, *58*, 380−388.

[37] [37a] M. Wilhelm, Doctoral Dissertation, University of Oldenburg, Germany, **2001**; also to be found under http://docserver.bis.uni-oldenburg.de/publikationen/dissertation/2001/wilneu01/wilneu01.html. [37b] H. Strasdeit, S. Deeken, W. Saak, M. Wilhelm, *GDCh-Jahrestagung Chemie 2001*, Würzburg, Germany, September 23−29, **2001**, Abstract WÖHLER-044. [37c] H. Strasdeit, M. Wilhelm, S. Deeken, E. Berssen, R. Koch, *35th Int. Conf. Coord. Chem.* Heidelberg, Germany, July 21−26, **2002**, Abstract P1.128.

[38] [38a] A. De Robertis, C. Foti, G. Patanè, S. Sammartano, *J. Chem. Eng. Data* **1998**, *43*, 957−960. [38b] D. L. Rabenstein, C. A. Evans, M. C. Tourangeau, M. T. Fairhurst, *Anal. Chem.* **1975**, *47*, 338−341. [38c] G. Schwarzenbach, M. Schellenberg, *Helv. Chim. Acta* **1965**, *48*, 28−46.

[39] [39a] C. A. Barradell, H. G. M. Edwards, D. N. Smith, *J. Organomet. Chem.* **1991**, *421*, 137−146. [39b] H. Schmidbaur, H.-J. Öller, S. Gamper, G. Müller, *J. Organomet. Chem.* **1990**, *394*, 757−764.

[40] R. S. Glass, G. S. Wilson, W. N. Setzer, *J. Am. Chem. Soc.* **1980**, *102*, 5068−5069.

[41] For a definition of the conformational nomenclature see: J. Dale, *Acta Chem. Scand.* **1973**, *27*, 1115−1129.

[42] A detailed conformational study of [9]aneS_3 in metal complexes is available: J. Beech, P. J. Cragg, M. G. B. Drew, *J. Chem. Soc., Dalton Trans.* **1994**, 719−729.

[43] [43a] P. Pyykkö, M. Straka, *Phys. Chem. Chem. Phys.* **2000**, *2*, 2489−2493. [43b] A. J. Canty, G. B. Deacon, *Inorg. Chim. Acta* **1980**, *45*, L225−L227. [43c] The possibility of a larger R_{vdW} value of Hg^{II} (around 2.0 Å) has been discussed, see for example: K. R. Flower, V. J. Howard, S. Naguthney, R. G. Pritchard, J. E. Warren, A. T. McGown, *Inorg. Chem.* **2002**, *41*, 1907−1912; S. S. Batsanov, *J. Chem. Soc., Dalton Trans.* **1998**, 1541−1545.

[44] Because van der Waals radii of sulfur and fluorine have been found to be anisotropic, ranges are used here instead of single values: S. C. Nyburg, C. H. Faerman, *Acta Crystallogr., Sect. B* **1985**, *41*, 274−279.

[45] S. C. Rawle, G. A. Admans, S. R. Cooper, *J. Chem. Soc., Dalton Trans.* **1988**, 93−96.

[46] R. E. DeSimone, M. D. Glick, *J. Am. Chem. Soc.* **1976**, *98*, 762−767.

[47] Only the non-disordered α and β_1 molecules of free [14]aneS$_4$ were used for comparison, see ref.[46]
[48] D. L. Rabenstein, *Acc. Chem. Res.* **1978**, *11*, 100−107.
[49] A. J. Canty, A. Marker, *Inorg. Chem.* **1976**, *15*, 425−430.
[50] [50a] P. L. Goggin, R. J. Goodfellow, D. M. McEwan, A. J. Griffiths, K. Kessler, *J. Chem. Res. (S)* **1979**, 194−195; *J. Chem. Res. (M)* **1979**, 2315−2343. [50b] K. Stanley, J. Martin, J. Schnittker, R. Smith, M. C. Baird, *Inorg. Chim. Acta* **1978**, *27*, L111−L113. [50c] H. Schmidbaur, K.-H. Räthlein, *Chem. Ber.* **1973**, *106*, 2491−2507.
[51] N. W. Alcock, N. Herron, P. Moore, *J. Chem. Soc., Dalton Trans.* **1978**, 394−399.
[52] See for example: H. Friebolin, *Basic One- and Two-Dimensional NMR Spectroscopy*, 3rd ed., Wiley-VCH, Weinheim, **1998**, p. 124f.
[53] K. E. Pitts, A. O. Summers, *Biochemistry* **2002**, *41*, 10287−10296.
[54] The numbering of the amino acid residues refers to the organomercurial lyase that is encoded by plasmid R831b, see ref.[53]
[55] T. Fujinaga, I. Sakamoto, *J. Electroanal. Chem.* **1977**, *85*, 185−201.
[56] F. A. L. Anet, D. J. O'Leary, *Tetrahedron Lett.* **1989**, *30*, 2755−2758.
[57] [57a] J. Pickardt, J. Shen, *Z. Naturforsch., Teil B* **1993**, *48*, 969−972. [57b] W. N. Setzer, Q. Guo, G. J. Grant, J. L. Hubbard, R. S. Glass, D. G. VanDerveer, *Heteroat. Chem.* **1990**, *1*, 317−325. [57c] A. J. Blake, A. J. Holder, T. I. Hyde, G. Reid, M. Schröder, *Polyhedron* **1989**, *8*, 2041−2045.
[58] C. Walsh, T. Begley, A. Walts, *Pure Appl. Chem.* **1987**, *59*, 295−298.
[59] For theoretical studies on mercury-second-row element complexes see: [59a] Ref.[30][59b]T. Rambusch, K. Hollmann-Gloe, K. Gloe, *J. Prakt. Chem.* **1999**, *341*, 202−217.
[60] For theoretical studies on Hg−C bond cleavage see: [60a] V. Barone, A. Bencini, F. Totti, M. G. Uytterhoeven, *Organometallics* **1996**, *15*, 1465−1469. [60b] V. Barone, A. Bencini, F. Totti, M. G. Uytterhoeven, *Int. J. Quantum Chem.* **1997**, *61*, 361−367. [60c] J. A. Tossell, *J. Phys. Chem. A* **1998**, *102*, 3587−3591.
[61] [61a] J. A. Altmann, N. C. Handy, V. E. Ingamells, *Int. J. Quantum Chem.* **1996**, *57*, 533−542. [61b] J. A. Altmann, N. C. Handy, *Phys. Chem. Chem. Phys.* **1999**, *1*, 5529−5536.
[62] M. Kaupp, *Chem. Ber.* **1996**, *129*, 535−544.
[63] G. Schreckenbach, T. Ziegler, *Theor. Chem. Acc.* **1998**, *99*, 71−82.
[64] [64a] M. Kaupp, O. L. Malkina, *J. Chem. Phys.* **1998**, *108*, 3648−3659. [64b] J. Vaara, O. L. Malkina, H. Stoll, V. G. Malkin, M. Kaupp, *J. Chem. Phys.* **2001**, *114*, 61−71.
[65] Review: J. Gauss, J. F. Stanton, *Adv. Chem. Phys.* **2002**, *123*, 355−422, and references cited therein.
[66] W. Kuechle, M. Dolg, H. Stoll, H. Preuss, *Mol. Phys.* **1991**, *74*, 1245−1263.
[67] [67a] P. C. Hariharan, J. A. Pople, *Mol. Phys.* **1974**, *27*, 209−214. [67b] M. M. Francl, W. J. Pietro, W. J. Hehre, J. S. Binkley, M. S. Gordon, D. J. DeFrees, J. A. Pople, *J. Chem. Phys.* **1982**, *77*, 3654−3665.
[68] M. B. Blayney, J. S. Winn, D. W. Nierenberg, *Chem. Eng. News* **1997**, *75*, 7.
[69] B. Wrackmeyer, R. Contreras, *Annu. Rep. NMR Spectrosc.* **1992**, *24*, 267−329.
[70] T. V. O'Halloran, C. P. Singer, *^{199}Hg NMR Standards*, to be found under http://www.chem.nwu.edu/~ohallo/HgNMRStandards/index.html, **1998**.
[71] The signal position was inferred from the proton-coupled ^{13}C NMR spectrum in which the CH_3 quadruplet is only partly superposed. The $^1J(^{13}C,^1H)$ values are 138.5 Hz ($HgCH_3$) and 143.9 Hz (CH_2).
[72] The isotopic pattern unambiguously showed that this signal was not due to $[(MeHg)_2([14]aneS_4)]^{2+}$.
[73] G. M. Sheldrick, *SHELX-97*, Universität Göttingen, Göttingen, Germany, **1997**.
[74] *DIAMOND−−Visual Crystal Structure Information System*, version 2.1, Crystal Impact, Bonn, Germany, **1999**.
[75] [75a] M. J. S. Dewar, E. G. Zoebisch, E. F. Healy, J. J. P. Stewart, *J. Am. Chem. Soc.* **1985**, *107*, 3902−3909. [75b] M. J. S. Dewar, Y. C. Yuan, *Inorg. Chem.* **1990**, *29*, 3881−3890. [75c] M. J. S. Dewar, C. Jie, *Organometallics* **1989**, *8*, 1547−1549.
[76] [76a] J. J. P. Stewart, *J. Comput. Chem.* **1989**, *10*, 209−220. [76b] J. J. P. Stewart, *J. Comput. Chem.* **1991**, *12*, 320−341.
[77] J. J. P. Stewart, *MOPAC 2002*, Fujitsu Limited, Tokyo, Japan, **2002**.
[78] M. J. Frisch, G. W. Trucks, H. B. Schlegel, G. E. Scuseria, M. A. Robb, J. R. Cheeseman, V. G. Zakrzewski, J. A. Montgomery, R. E. Stratmann, J. C. Burant, S. Dapprich, J. M. Millam, A. D. Daniels, K. N. Kudin, M. C. Strain, O. Farkas, J. Tomasi, V. Barone, M. Cossi, R. Cammi, B. Mennucci, C. Pomelli, C. Adamo, S. Clifford, J. Ochterski, G. A. Petersson, P. Y. Ayala, Q. Cui, K. Morokuma, D. K. Malick, A. D. Rabuck, K. Raghavachari, J. B. Foresman, J. Cioslowski, J. V. Ortiz, B. B. Stefanov, G. Liu, A. Liashenko, P. Piskorz, I. Komaromi, R. Gomperts, R. L. Martin, D. J. Fox, T. Keith, M. A. Al-Laham, C. Y. Peng, A. Nanayakkara, C. Gonzalez, M. Challacombe, P. M. W. Gill, B. G. Johnson, W. Chen, M. W. Wong, J. L. Andres, M. Head-Gordon, E. S. Replogle, J. A. Pople, *GAUSSIAN*, Gaussian, Inc., Pittsburgh, PA, USA, **1998**.
[79] [79a] T. H. Dunning, Jr., P. J. Hay in *Modern Theoretical Chemistry*, vol. 3 ("Methods of Electronic Structure Theory") (Ed.: H. F. Schaefer, III), Plenum, New York, **1977**, p. 1−27. [79b]P. J. Hay, W. R. Wadt, *J. Chem. Phys.* **1985**, *82*, 270−283.
[80] [80a] A. D. Becke, *Phys. Rev. A* **1988**, *38*, 3098−3100. [80b] J. Perdew, *Phys. Rev. B* **1986**, *33*, 8822−8824. [80c] J. Perdew, *Phys. Rev. B* **1986**, *34*, 7406.
[81] C. Lee, W. Yang, R. G. Parr, *Phys. Rev. B* **1988**, *37*, 785−789.
[82] A. D. Becke, *J. Chem. Phys.* **1993**, *98*, 5648−5652.

Received December 5, 2003
Early View Article
Published Online April 7, 2004

